CARBON 49 (2011) 3762–3772

available at www.sciencedirect.com

ScienceDirect

journal homepage: www.elsevier.com/locate/carbon

Lysine-assisted rapid synthesis of crack-free hierarchical carbon monoliths with a hexagonal array of mesopores

Guang-Ping Hao [a], Wen-Cui Li [a], Shuai Wang [a], Guang-Hui Wang [a], Lin Qi [b], An-Hui Lu [a,*]

[a] State Key Laboratory of Fine Chemicals, School of Chemical Engineering, Dalian University of Technology, Dalian 116024, PR China
[b] School of Materials Engineering, Dalian University of Technology, Dalian 116024, PR China

ARTICLE INFO

Article history:
Received 20 March 2011
Accepted 6 May 2011
Available online 11 May 2011

ABSTRACT

The rapid and scalable synthesis of hierarchical carbon monoliths with an ordered mesostructure and fully interconnected macropores has been demonstrated. Resorcinol and formaldehyde based polymers were used as the carbon precursor, triblock copolymer Pluronic F127 as the structural directing agent, and organic base lysine as both the polymerization catalyst and mesostructure assembly promoter. In the presence of lysine, homogeneous and crack-free polymer monoliths can be obtained through rapid gelation in 15 min at 90 °C. The polymer monoliths have a robust framework, which can be directly dried at 50 °C in air and carbonized at high temperature under a nitrogen atmosphere. The carbon monoliths are crack-free and have an ordered mesostructure with fully interconnected macropores. The surface area and the macropore volume are high with values up to 600 $m^2 g^{-1}$ and 3.52 $cm^3 g^{-1}$, respectively. Further steam activation of the carbon monolith can significantly improve the surface area to 2422 $m^2 g^{-1}$ while still maintaining the ordered mesostructure.

1. Introduction

Development of time-saving and scalable synthesis of hierarchical carbon monoliths with an ordered mesostructure has been on the long wishing list [1–8]. The so far reported syntheses usually require either long operation time, large amount of solvent exchange and supercritical drying [9], or many synthesis steps [10], or careful thin film preparation and solvent drying [11–13]. Moreover, these methods are often difficult to obtain monoliths with ordered mesostructures. Compared with the methods mentioned above, nanocasting pathway is a straight forward way to prepare monolithic carbons with ordered mesostructures [14–18]. This method usually involves several steps such as preparation of a crack-free silica monolith template, impregnation and polymerization of a carbon precursor, carbonization and removal of the silica template. This process is uneconomic to scale up. Thus, it is challenging to explore an easy and scalable synthesis of hierarchical carbon monoliths with an ordered mesostructure.

A direct soft-template method based on supramolecular assemblies of surfactants and carbon precursors is regarded as an alternative option. At present, its products are mostly in a form of powder or film [19–28]. For example, an oriented mesoporous carbon film was prepared through a solvent annealing accelerated self-assembly method using polystyrene-block-poly (4-vinylpyridine) (PS-P4VP) as soft templates and *N*, *N*-dimethylformamide (DMF) as the solvent [22]. Soon later, a hexagonal mesoporous carbon film was prepared through a spin coating method using resorcinol–formaldehyde copolymer and triethylorthoacetate (EOA) as the coprecursor, F127 as the template and HCl (5M) as the catalyst [23]. Using an evaporation induced self-assembly method, ordered mesoporous carbon films have been prepared either with an EO–PO–EO/resol system in which the pH value is near

* *Corresponding author:* Fax: +86 411 84986112.
E-mail address: anhuilu@dlut.edu.cn (A.-H. Lu).
0008-6223/$ - see front matter
doi:10.1016/j.carbon.2011.05.010

neutral [24,25], or with a resorcinol–formaldehyde-F108 system under basic (NaOH) conditions [26]. Recently, using organo-catalyst glutamic acid instead of the conventional inorganic catalysts such as NaOH and HCl, ordered mesoporous carbons were prepared by the self-assembly resorcinol–formaldehyde-F127 system [29]. The particular feature of this synthesis is that no any inorganic compounds were involved, thus high purity carbon can be achieved.

Only very recently, based on the soft-templating principle, monolithic carbons with ordered mesopores have been prepared by either the combination of centrifugation and shaping techniques [30,31] or the polymerization-induced spinodal decomposition in glycolic solutions [32], or a hydrothermal approach [33,34]. To form a polymer framework, the above synthesis usually took several hours at least, or even longer, basically by using an inorganic catalyst (HCl or NaOH). The carbon framework obtained consists of carbon, oxygen and hydrogen. However, nitrogen-containing carbon framework is practically more desirable in the applications of catalysis, electrochemistry and adsorption [35–39].

Herein, we report a rapid and scalable synthesis of crack-free and nitrogen-doped carbon monoliths with fully interconnected macropores and an ordered mesostructure through the soft-template method. The monoliths are achieved by using organic base lysine as a polymerization agent and mesostructure assembly promotor, through rapid sol– gel process in about 15 min at 90 °C.

2. Experimental

2.1. Synthesis of ordered mesoporous monolithic carbons

In a typical synthesis procedure of hierarchical carbon monolith (e.g. HCM-1), 3.0 g resorcinol (27.3 mmol) and 1.25 g Pluronic F127 were dissolved in 18 g solvent mixture of ethanol (11.4 ml) and water (9 ml) with magnetic stirring at 25 °C. Afterwards, 0.3 g L-lysine (2.1 mmol) was added to the above solution and stirred for about 30 min at 25 °C till the solution turned pale yellow. Subsequently, 4.42 g formalin (37 wt.%) containing formaldehyde (1.64 g, 54.5 mmol) was quickly injected into the pale yellow solution. The reaction system instantaneously (less than 1 min) turned to white homogeneous emulsion, and the reaction mixture was stirred at 25 °C for another 10 min. Then the white homogeneous emulsion system was sealed and transferred into oven at 90 °C. It solidified within 15 min and was cured for 2–4 h. The monoliths were prepared by varying the molar ratios of the reactants (resorcinol, F127, lysine, see Table 1), while maintaining the molar ratio of resorcinol to formaldehyde 1:2, and the volume ratio of water to ethanol 0.79:1. Due to the quick gelation of the reaction system immediately after adding formalin, the pH value is thus difficult to measure. Instead, it was measured before adding formalin (see Table 1). The pH of the formalin solution is 4.53.

The as-made polymer monoliths were dried at 50 °C for 24 h. They were then pyrolysed under a nitrogen atmosphere, thus to obtain crack-free carbon monoliths. The pyrolysis temperature increased to 400 °C with a heating rate of 2 °C min^{-1} and held at that temperature for 1 h. Subsequently, the temperature was increased to 800 °C (only HCM-1 was heated to 500 °C) with a heating rate of 5 °C min^{-1} and maintained at that temperature for 2 h. Finally the furnace was naturally cooling down to room temperature.

Table 1 – Synthesis conditions in the polymerization procedure.

Sample	pH	Solid content %	Molar ratio of		
			Resorcinol:	Lysine:	F127
HCM-1[a]	8.92	30	275	20	1
HCM-2[b]	8.92	30	275	20	1
HCM-3[c]	8.92	30	275	20	1
HCM-4	8.72	20	275	20	1
HCM-5	9.34	40	275	20	1
HCM-6	9.14	30	275	34	1
HCM-7	9.26	30	275	55	1
HCM-8	9.02	30	137	20	1
HCM-9	8.99	30	191	20	1
HCM-10	9.05	30	429	20	1
HCM-11	9.03	30	687	20	1

[a] HCM-1 and HCM-2 were prepared by the carbonization of the same starting polymer monolith. HCM-1 was carbonized at 500 °C.
[b] HCM-2 was carbonized at 800 °C.
[c] HCM-3 was obtained by steam activation of HCM-2 at 850 °C for 1 h.

2.2. Characterization

Transmission electron microscopy (TEM) images of the samples were obtained with a Tecnai $G^2$20S-Twin electron microscope equipped with a cold field emission gun. The acceleration voltage was 200 kV. Samples were prepared by dropping a few drops of a suspension of one sample in ethanol onto the holey carbon grid with a pipette. Scanning electron microscope (SEM) investigations were carried out with a Hitachi S-4800 instrument. The X-ray diffraction (XRD) measurements were taken on a Rigaku D/Max 2400 diffractometer using CuK_α radiation (40 kV, 100 mA, $\lambda = 0.15406$ nm). The d spacing values were calculated by the formula $d = \lambda/2\sin\theta$, and the unit cell parameters were calculated from the formula $a_0 = 2d_{100}/\sqrt{3}$. Nitrogen sorption isotherms were measured with a TriStar 3000 adsorption analyzer (Micromeritics) at liquid nitrogen temperature. The Brunauer–Emmett–Teller (BET) method was utilized to calculate the specific surface areas (S_{BET}). Pore size distributions (PSDs) were derived from the adsorption branches of the isotherms using the Barrett–Joyner–Halenda (BJH) model. (The isotherms have the closure of the hysteresis around $P/P_0 = 0.42$, due to the instability of a meniscus. In this case, using the desorption branch to calculate the pore sizes would lead to an untrue reflection of the PSDs. Thus, the adsorption branches were used to determine the PSDs in here.) The total pore volumes were estimated from the adsorbed amount at a relative pressure P/P_0 of 0.997. Micropore volume (V_{micro}) was calculated using the t-plot method. Mesopore volume (V_{meso}) was calculated from the difference of the total pore volume and the micropore volume. Hg intrusion isotherms and pore-size distributions of the pores larger than 50 nm were measured using a Micromeritics AutoPore IV 9500 analyzer. Elemental analysis was carried out

on a CHNO elemental analyzer (Vario EL III, Elementar). $^{1}H \rightarrow {}^{13}C$ cross-polarization magic-angle-spinning (CP/MAS) NMR experiments were performed on a Varian Infinityplus-400 spectrometer equipped with a 5 mm MAS probe. The spectra were recorded at 100.5 MHz with a spinning rate of 11 kHz, 2000–3600 scans, a contact time of 3 ms, and a recycle delay of 4 s. The chemical shifts of ^{13}C NMR spectra were referenced to tetramethylsilane. Before the CP/MAS NMR measurements, the as-synthesized polymer monolith was ground into fine powders.

3. Results and discussion

3.1. Synthesis principle

As illustrated in Fig. 1, the key factor for rapid synthesis of the polymer monolith is the selection of L-lysine for initiating the polymerization and self-assembly. Lysine molecules can form intra-molecule salt, so the deprotonated carboxyl group and the protonated NH_3^+ group can form hydrogen bonds with the –OH group of resorcinol and the hydrophilic EO (N–H···O) segment of EO_{106}–PO_{70}–EO_{106}. It is expected that the lysine molecule would enhance the assembly of the mesostructure between F127 and resorcinol–formaldehyde. In addition, lysine is a basic amino acid, which can provide basic environment for the polymerization of resorcinol and formaldehyde. Lysine participates in the polymerization and mesostructure assembly, leading to the formation of a hybrid composite which consists of poly (RF) resin, polybenzoxazine (RF-lysine) resin and block copolymer, as evidenced by the $^{1}H \rightarrow {}^{13}C$ CP/MAS NMR analyses below in Fig. 4.

As expected, a fast gelation (polymerization + assembly) is completed within 15 min at 90 °C, when the molar ratio of these reactants of Resorcinol/Formaldehyde/Lysine/F127/H_2O/EtOH was set as 275/500/20/1/4945/1978. In contrast, without lysine, the gelation period would require at least 8 h long. As shown in Fig. 1 (photographs), after mixing all reactants, the reaction solution instantaneously turned to a white homogeneous emulsion, whereas without lysine, the solution retains clear and transparent. This indicates the reaction was quickly triggered by lysine molecules. The resultant prepolymer solution was stirred at 25 °C for another 5 min, and then transferred to a 90 °C oven. The reaction system soon turns to pale yellow and continues to deepen its color to dark yellow, revealing that the polymerization and mesostructure assembly take place further. Such appearances are sharply different from that of the reported processes without using lysine [22,24,26,30]. Hence, the quick color changes in the current system evidently prove the important function of lysine in such rapid polymerization and self-assembly process. With such a rapid solidification of the gel, the micelles evolving from assembled F127 molecules are fixed in the polymer framework, which would result in the formation of an ordered mesostructure. It should be pointed out that during the entire synthesis, the whole gel (see Fig. 1) was homogeneous in appearance and no sedimentation or macroscopic phase separation was observed. This is different from previous reports in which macroscopic phase separation (or polymer precipitation) often occurred [26,27]. Compared with the conventional drying processes for monolith polymer (e.g. supercritical or subcritical drying, or solvent evaporation), the remarkable advantage of the present synthesis is that the as-made polymer monolith can be dried directly in air

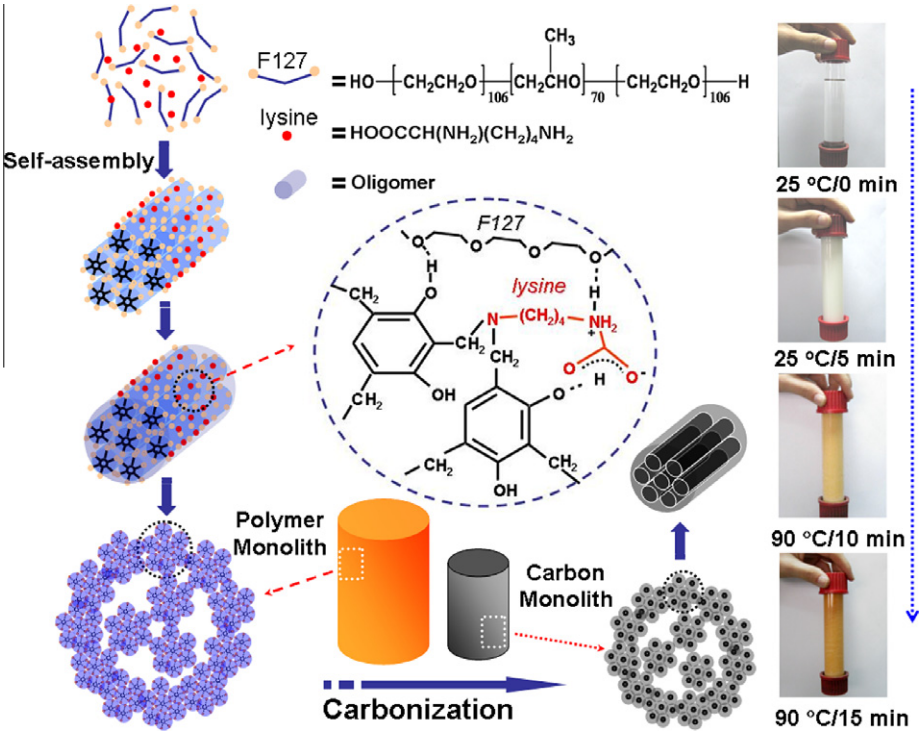

Fig. 1 – Schematic of the rapid synthesis of N-doped a hierarchically porous carbon monolith with an ordered mesostructure.

at 50 °C to form the crack-free monolithic material. The current drying process is time-saving and much easy to operate.

Since the triblock copolymer template can decompose completely when the pyrolysis temperature is higher than 350 °C, one polymer monolith was thus carbonized at 500 °C and the obtained carbon monolith was denoted as HCM-1. Elemental analysis reveals that the carbon monolith HCM-1 consists of 0.58% N, 79.30% C, 2.94% H and 17.18% O (by weight). The N species is derived from amino acids, as demonstrated before [40]. Noticeably, N-doped carbons have been proven to possess several advantages. For example, it is known that the introduction of the N heteroatom into the graphitic structure contributes further electron carriers in the conduction band [36]. In addition, the N-containing Lewis basic sites can bind acid molecules, such as CO_2 [38,39].

The carbon monolith HCM-1 was further characterized with SEM, Hg intrusion, XRD, TEM and N_2 sorption. As shown in Fig. 2a, the crack-free polymer monolith was currently

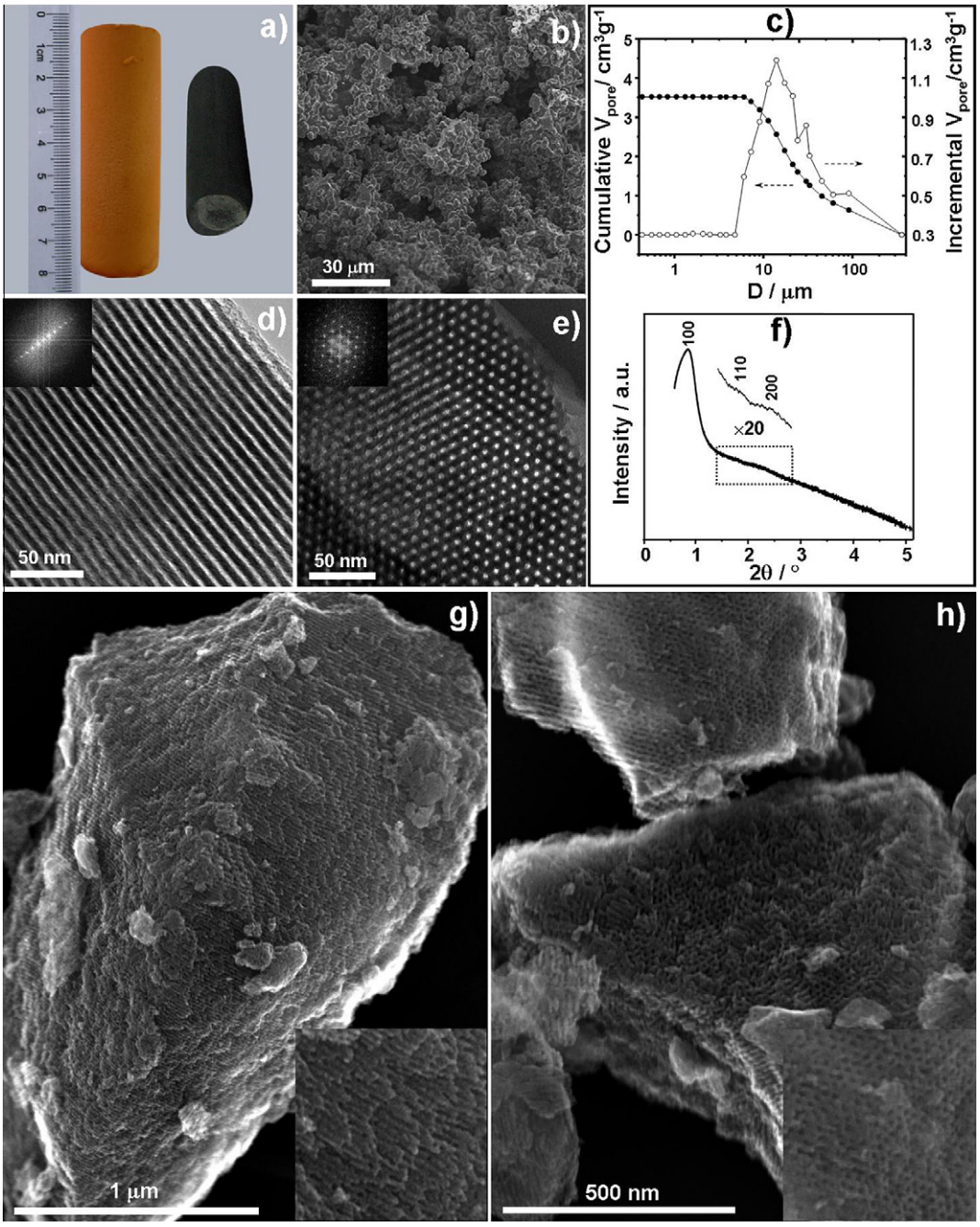

Fig. 2 – Characterizations of HCM-1: (a) representative photos of the polymer and carbon monolith, (b) SEM image, (c) Hg intrusion curve and differential pore diameter distribution, (d) TEM image and FFT diffractogram (inset) viewed in the [1 1 0] direction, (e) TEM image and FFT diffractogram (inset) viewed in the [0 0 1] direction, (f) low-angle XRD pattern, (g) and (h) SEM images with low and high (inset) magnification viewed perpendicular to and parallel to the pore channels.

prepared with the length and diameter of 70 and 20 mm, respectively. The sizes depend on the container during the gelation step. Following a carbonization process, a crack-free carbon monolith is obtained with the sizes of 51 mm in length and 15 mm in diameter. The volume shrinkage is ca. 59%. The mechanical strength test shows that the carbon monolith can bear a pressure of ~0.3 MPa. The SEM image (Fig. 2b) displays that carbon monolith HCM-1 exhibits fully interconnected, sponge-like macropores. The carbon framework is consisting of fused carbon particles with the size ca. 1.5 μm. Hg intrusion is a bulk method that probes the whole sample opposite to what is the case in microscopy investigations. Hg intrusion (Fig. 2c) data shows a continuous increase in Hg uptakes until the pore diameter reaches ca. 7.4 μm. The macropore sizes are concentrated around 15 μm. The abundant fully interconnected macroporoes endow a large total volume of 3.52 $cm^3 g^{-1}$. These values are much larger than those (macropore size 3 μm, macropore volume 1.14 $cm^3 g^{-1}$) reported previously [33].

Moreover, the TEM image (Fig. 2d) recorded perpendicularly to the direction of the pore channels, exhibits well-organized parallel channels. The thickness of the pore wall is estimated as 6.8 nm. TEM images (Fig. 2e) show that a hexagonally ordered array of circles can be clearly observed in the direction parallel to the pore channels. The center-to-center distances of adjacent channels are ca. 12.9 nm. This together with the Fast Fourier transform (FFT) diffractograms (inset) indicate ordered meosporous structure with hexagonal (*p6mm*) symmetry. The low-angle XRD pattern of HCM-1 (Fig. 2f) shows one strong and two visible peaks, which can be indexed as (1 0 0), (1 1 0) and (2 0 0) reflections based on hexagonal symmetry (*p6mm*). The intense (1 0 0) peak corresponds to a d-spacing of 11.3 nm, from which a unit cell parameter is calculated as 13.1 nm, which is almost identical to the distance estimated from the TEM observation. High resolution SEM images (Fig. 2g and h) viewed perpendicular to and parallel to the mesopore channels further confirm that carbon monolith HCM-1 exhibits a long-range and large domain 2D hexagonal arrangement, which are consistent with the results of TEM and XRD.

In fact, the carbonization temperature imposes an important effect on the mesostructures of the carbon product. Following HCM-1 carbonized at 500 °C, the same polymer monolith was further carbonized at 800 °C and the product was named as HCM-2. Fig. 3 shows the characterization results of sample HCM-2. The Hg intrusion (Figs. 2c and 3a) data shows that the macropore volume decreases from 3.52 to 2.12 $cm^3 g^{-1}$ and the average macropore size decreases from 15 to 10 μm when the carbonization temperature increases from 500 °C to 800 °C. The XRD pattern (Fig. 3b) of HCM-2 shows well-resolved reflections, which can be indexed as (1 0 0), (1 1 0) and (2 0 0) reflections, based on hexagonal symmetry (*p6mm*). TEM images (Fig. 3c and d) show a good 2D hexagonal *p6mm* symmetry. The unit cell parameter, a_0, of HCM-2 is 11.9 nm as calculated based on the XRD pattern, which is consistent with that of TEM analysis. It is identified that the lattice shrinkage was as large as 9.2% when carbonization temperature increased from 500 °C to 800 °C.

The N_2 sorption isotherms (Fig. 3e) of both HCM-1 and HCM-2 yield type-IV curves with a sharp capillary condensation step at P/P_0 = 0.6–0.7 and a H1-type hysteresis loop, which is a typical characteristic of mesoporous materials with cylindrical channels. The mesopore sizes are around 6.3 nm for HCM-1 and 5.4 nm for HCM-2. As seen in Table 2, the specific surface areas are 600 and 654 $m^2 g^{-1}$ for HCM-1 and HCM-2, respectively. The high carbonization temperature leads to a decrease in the pore size and the pore volume due to the structural thermal shrinkage, but a slight increase in the specific surface area due to the fully decomposition of the polymer framework. Even when the synthesis was scaled up by a factor of 30, its product still maintained a perfect monolith shape and exhibited nearly identical mesostructures with the specific surface area, pore volume and mesopore size of 598 $m^2 g^{-1}$, 0.39 $cm^3 g^{-1}$ and 5.5 nm, respectively.

Steam activation is a conventional method to create porosity of carbon materials. The abundant macro- and mesoporosity in the carbon monolith will facilitate the diffusion of steam throughout this material, thus an easy activation will preferentially improve the micropores by the reaction between steam and carbon. In order to further increase the surface area meanwhile to test the stability of the ordered mesostructure, sample HCM-2 was activated by steam at 850 °C for 1 h and the product was named as HCM-3. Low angle XRD pattern (Fig. 3b) of the HCM-3 shows resolved reflections corresponding to a hexagonal symmetry (*p6mm*), indicating the original ordered mesostructure was retained after steam activation. The N_2 sorption isotherm of HCM-3 (Fig. 3f) is belonging to type IV, with a more significant nitrogen uptake at the relative pressure lower than 0.1. Its BET surface area and mesopore volume are high with values up to 2422 $m^2 g^{-1}$ and 1.03 $cm^3 g^{-1}$, respectively (see Table 2). This indicates an intensive etching of the ordered mesopore walls by water molecules at 850 °C, thus to decrease the density of the carbon framework in turn to increase the pore volume. However, the average mesopore size is ca. 5.6 nm, which is very close to that of HCM-2. Obviously, the steam activation mainly creates microporosity within the carbon pore walls rather than enlarges the mesopores by elimination of the mesopore walls.

As discussed above, the unique carbon monoliths were the highly desired product with abundant interconnected macropores and ordered mesopores. Here, $^1H \rightarrow {}^{13}C$ CP/MAS NMR technique was employed to understand the role of lysine in the synthesis. The spectra are presented in Fig. 4. HPM-1 represents the polymeric sample corresponding to the carbonaceous product HCM-1 listed in Table 1. The sample RF-NaOH and RF-Lysine [40] represent correspondingly NaOH and lysine catalyzed resorcinol–formaldehyde polymeric products (without F127 used), which were used as control samples. Based on the ^{13}C NMR spectrum of lysine in the literatures [41,42], we could assign these characteristic peaks (at 174, 55 and 30 ppm) derived from lysine in the samples, HPM-1 and RF-Lysine. The resolved peaks at ~55 ppm are assigned to the signal of the carbon in Ar–CH_2–N–, and the peaks at ~30 and ~26 ppm are the signals of the carbons in –$(CH_2)_4$–NH_2; while the clear peaks at ~174 ppm are attributed to the carbon in the –COO^- groups, which derived from lysine. By comparing the spectra of the HPM-1 with those of RF-Lysine and RF-NaOH (without F127 used), the unique signals at ~72 and ~18 ppm can be identified as the carbons in the methylene and methyl groups of the block

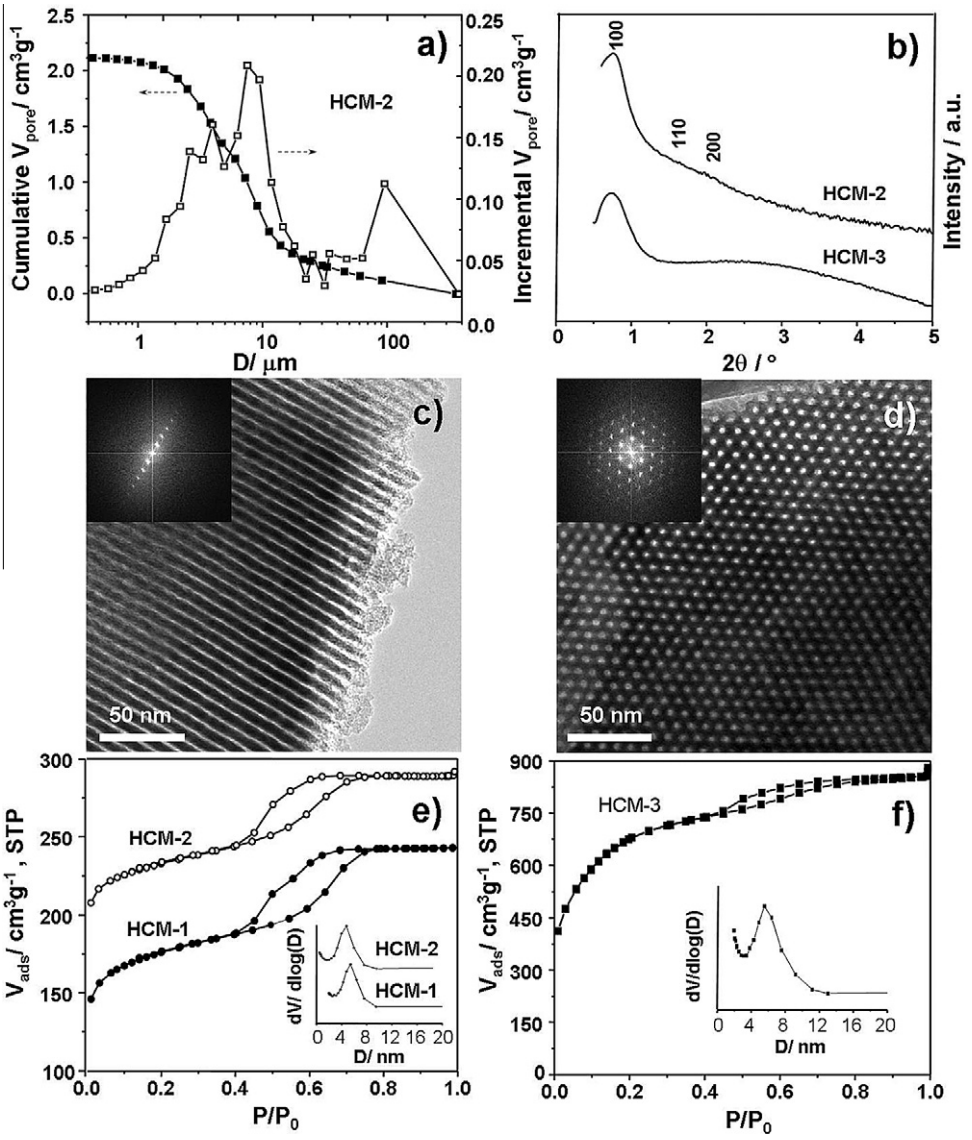

Fig. 3 – (a) Hg intrusion curve and pore diameter distribution of HCM-2, (b) low-angle XRD patterns of HCM-2 and HCM-3, (c) and (d) TEM images and their corresponding FFT diffractograms (inset) of HCM-2 viewed in the [1 1 0] and [0 0 1] direction, respectively, e) N_2 isotherms of HCM-1 and HCM-2 and their corresponding PSDs (inset), the isotherm of HCM-2 is offset vertically by 40 cm^3 g^{-1}, (f) N_2 isotherm and its PSD (inset) of HCM-3 activated by steam at 850 °C.

copolymer F127 template [25,43]. The strong and broad signals with chemical shifts ranging from 100 to 160 ppm are attributed to carbons in the aromatic rings of resorcinol–formaldehyde or resorcinol–formaldehyde–lysine polymer networks. The broad overlapping signals at ~26 ppm could also be attributed to the methylene linkages between aromatic rings. Hence, the $^1H \rightarrow {}^{13}C$ CP/MAS NMR results, together with the above elemental analysis, confirm that lysine participates in the polymerization leading to the formation of the hybrid composite (HPM-1) which consists of poly (RF) resin, polybenzoxazine (RF-lysine) resin and block copolymer.

3.2. *Influence of solid contents*

In the experiments, the ethanol–water solution (weight ratio of 1:1) was used to prepare hierarchically porous carbon monolith. The solid content (mass ratio between reactant and solvent) is an important factor to control the microstructure of carbon materials. Therefore, the influence of solid content on the mesostructure of carbon monolith was investigated. By maintaining the same molar ratio of lysine to F127 as that of sample HCM-2, but varying the amount of the solvent, a series of carbon products were obtained. Macroscopically, when the solid content is lower down to 20%, the obtained polymer and carbon monolith (HCM-4) are quite fragile and can be easily broken into small pieces. However, the carbon monolith maintains ordered mesostructures according to the TEM image (Fig. 5a) and the XRD result (Fig. 5b). It gives a type IV nitrogen sorption isotherm (Fig. 5c) with a visible hysteresis loop over the relative pressure, P/P_0, ranging from 0.4 to 0.8, which is similar to that of HCM-2. However, a high solid content up to 40% leads to a

Table 2 – Texture parameters of the hierarchical carbon monoliths.

Sample	S_{BET}[a]/$m^2\ g^{-1}$	D_{meso}[b]/nm	V_{micro}[c]/$cm^3\ g^{-1}$	V_{meso}[d]/$cm^3\ g^{-1}$
HCM-1	600	6.3	0.19	0.22
HCM-2	654	5.4	0.23	0.16
HCM-3	2422	5.6	0.27	1.03
HCM-4	605	5.3	0.19	0.23
HCM-5	756	–	0.31	0.07
HCM-6	565	6.1	0.21	0.14
HCM-7	593	14.9	0.24	0.12
HCM-8	640	6.0	0.24	0.17
HCM-9	695	6.0	0.24	0.26
HCM-10	568	4.8	0.20	0.13
HCM-11	554	3.9	0.22	0.07

[a] Apparent surface area calculated by multipoint BET method at the relative pressure range of 0.05–0.30.
[b] Pore sizes at maxima of the PSDs calculated based on the adsorption branch using BJH method.
[c] Micropore volume (V_{micro}) was calculated using the *t*-plot method.
[d] Mesopore volume (V_{meso}) was calculated from the difference of the total pore volume and the micropore volume. The total pore volumes were estimated from the adsorbed amount at a relative pressure P/P_0 of 0.997.

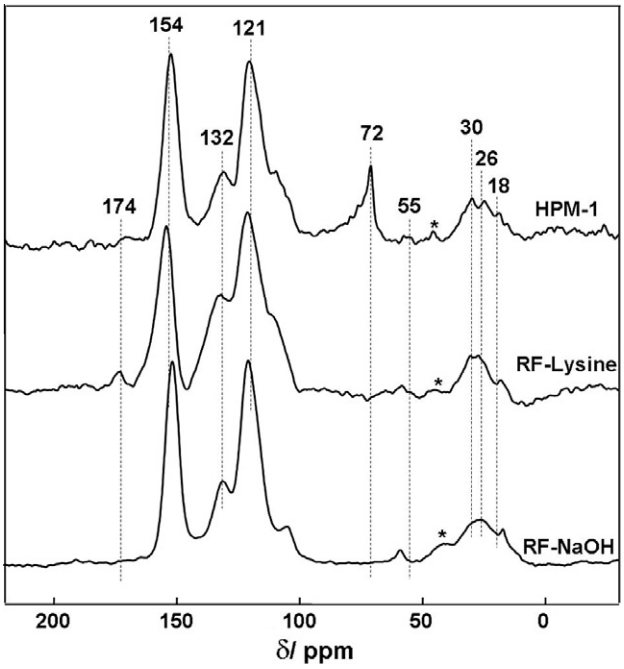

Fig. 4 – $^1H \rightarrow {}^{13}C$ CP/MAS NMR spectra of the as-made polymer monoliths: HPM-1 (lysine + F127), RF-NaOH (NaOH catalyzed) and RF-Lysine (lysine catalyzed). Asterisk denotes the spinning sidebands.

formation of disordered carbon monolith (HCM-5). The isotherm of HCM-5 is essentially type I, indicating microporous feature.

We have also investigated the use of pure solvents either water or ethanol for synthesis of the ordered mesoporous carbon. When only water is used for dissolving of F127, a large amount of foams formed under magnetic stirring. Finally no homogeneous product was obtained. When only ethanol is used, the dissolution of F127 and lysine requires a much longer period at room temperature, meanwhile the product is powder material. Hence, it is important to use the ethanol–water solution as the solvent for the dissolution of the reactants.

3.3. *Influence of the amount of lysine*

As lysine plays an important role in the synthesis of the hierarchical carbon monolith with ordered mesostructures, the influence of the amount of lysine on the formation of such ordered carbon monoliths was investigated (see Table 1, sample HCM-2, HCM-6 and HCM-7). For example, when the molar ratio of Resorcinol:Lysine:F127 < 275:20:1 was used, a macroscopic phase separation phenomenon occurs, i.e. a solvent-rich region and a polymer-rich region are observed. Under this synthesis condition, the obtained sample is thus nonuniform. When the molar ratio of Resorcinol:Lysine:F127 was controlled as 275:20:1, as discussed before, the carbon monolith HCM-2 exhibited well-organized mesostructure. When the molar ratio of Resorcinol:Lysine:F127 is 275:34:1, the carbon monolith HCM-6 with mesoporosity was obtained. However, the TEM image (Fig. 6a) and XRD pattern (Fig. 6b) reveal the coexisting of ordered and worm-like mesopores. When the molar ratio of Resorcinol:Lysine:F127 $\geq$ 275:55:1 was used, the polymer monolith was quickly formed within 3 min after mixing the reactants together. Unfortunately, the obtained carbon monolith HCM-7 dominantly exhibits micropores and macropores instead of mesopores (see Fig. 6c).

As seen in Table 1, the increased amount of lysine did not result in obvious changes of the pH values of the reaction solution. However, the amount of lysine is indeed very important for determining the mesostructure of the carbon monolith. The lower amount of lysine could result in the assembly of polymer species around F127 micelles. However, the assembly and growth of the building units is much quicker than the cross-linking of the assembled units, resulting in sedimentation. In another case, no ordered mesostructures were achieved, since the larger amount of lysine results in faster condensation and cross-linking of resorcinol and formaldehyde than the assembly of RF polymer around the micelles of F127. Hence, the formation of a monolithic structure with desired mesostructure requires a match in the reaction rate of

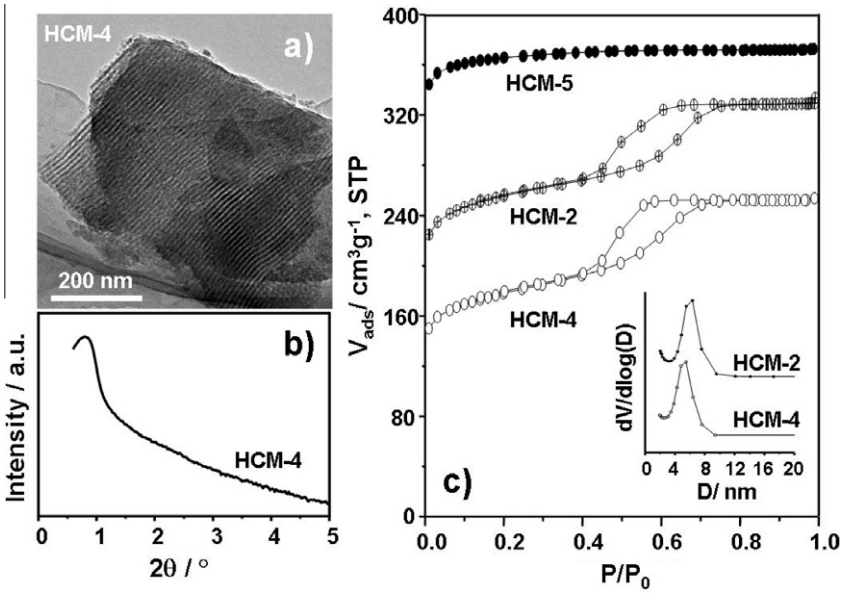

Fig. 5 – (a) TEM image and (b) low angle XRD pattern of HCM-4, and (c) nitrogen sorption isotherms of HCM-2, HCM-4 and HCM-5 synthesized with the mass content of 30%, 20% and 40% and corresponding PSDs (inset), offset vertically: HCM-2 by 60 cm^3 g^{-1}, HCM-5 by 100 cm^3 g^{-1}, STP.

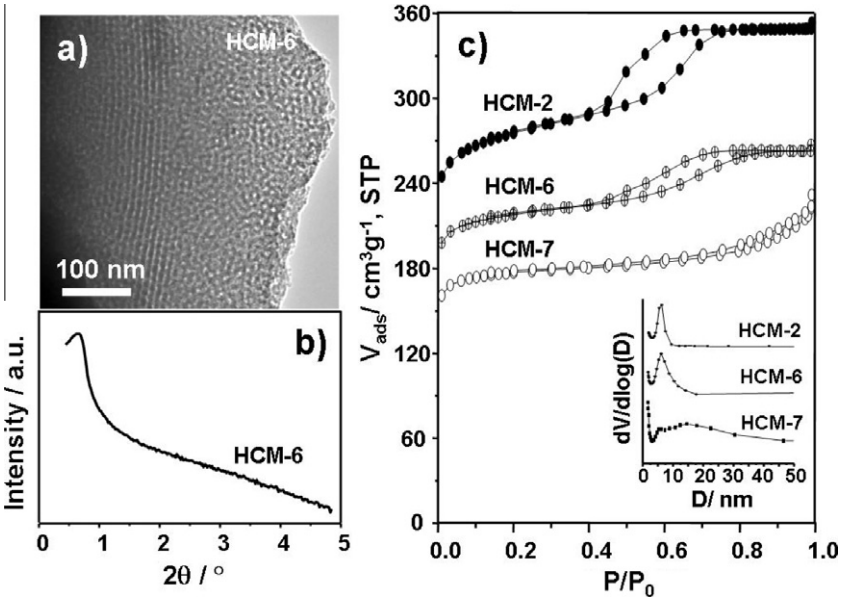

Fig. 6 – (a) TEM image and (b) low angle XRD pattern of HCM-6, and (c) nitrogen sorption isotherms of HCM-2, HCM-6 and HCM-7 synthesized with the R:Lysine:F127 M ratios of 275:20:1, 275:34:1 and 275:55:1 and the corresponding PSDs (inset), offset vertically: HCM-2 by 100 cm^3 g^{-1}, HCM-6 by 50 cm^3 g^{-1}.

the polymerization of resorcinol and formaldehyde, assembly of polymer species around F127 micelles, and the cross-linking of the mesostructure units.

Besides lysine, other amino acids such as L-arginine (Arg) and L-glutamine (Glu) were also used for the preparation of monolithic carbons. Following the best synthesis conditions of sample HCM-2, the amount of the amino acids were adjusted to achieve a pH value of the reaction solutions (without adding formalin) close to that of HCM-1. The results show that using Arg and Glu as the polymerization catalysts, there is no ordered mesostructures in the resultant carbons. We have varied the pH value (from 8.7 to 9.1) of the reaction system by changing the amount of Arg meanwhile retaining the other synthesis parameters, however, there is still no ordered mesostructures.

3.4. *Influence of the amount of F127*

It is known that self-organized arrays of non-covalently associated amphiphiles may exist as self-supported lamellar/vesicular, various bicontinuous cubic, or hexagonal/cylindrical phases when the concentration of the amphiphiles changes [44,45]. In the present study, the amounts of F127

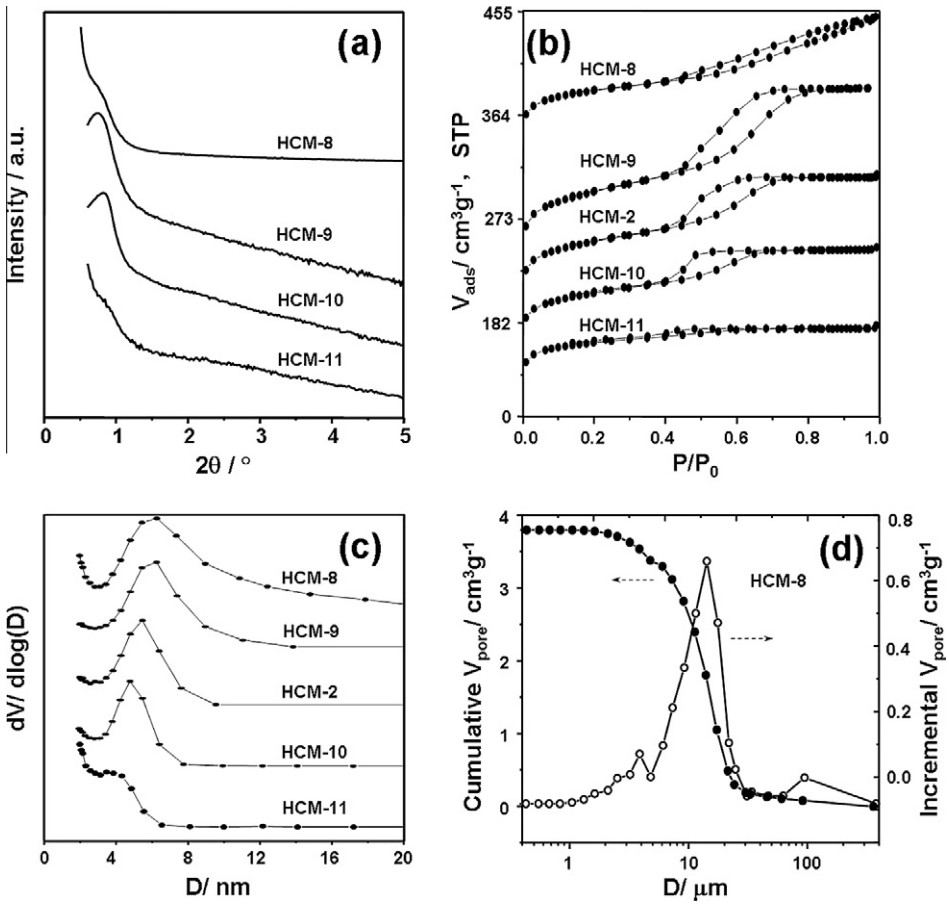

Fig. 7 – (a) Low-angle XRD patterns of samples from HCM-8 to HCM-11, (b) and (c) N_2 isotherm of samples HCM-2, HCM-8 to HCM-11 and the corresponding PSDs, The isotherms of HCM-2, HCM-8, HCM-9 and HCM-10 were vertically offset by 60, 200, 100 and 40 cm^3 g^{-1}, respectively, (d) Hg intrusion curve and differential pore diameter distribution of HCM-8.

have been varied in order to examine its effects on the formation of mesostructures in the carbon monoliths. Here, the molar ratio of resorcinol:F127 was used as index to describe the concentration of the template agent.

As seen in Table 1, sample HCM-n (n = 8, 9, 2, 10, 11), crack-free and cylindrical shape carbon monoliths can be prepared under different molar ratios of resorcinol:F127 = 137:1, 191:1, 275:1, 429:1 and 687:1, respectively. The XRD patterns of samples from HCM-8 to HCM-11 are shown in Fig. 7a. The XRD patterns of HCM-8 and HCM-11 show less-resolved reflections as compared with other samples, reflecting that these two samples exhibit a certain mesoporous feature with less ordered mesostructures. It indicates the order degree is dependent on the F127 concentration. With the molar ratio of resorcinol:F127 was set as moderate values of 191:1, 275:1 and 429:1, respectively, the products HCM-9, HCM-2 (see Fig. 3b) and HCM-10 show well-organized mesostructures.

The N_2 sorption isotherms of the series of samples and their corresponding PSDs are shown in Fig. 7b and c. The isotherm of HCM-11 with lowest concentration of F127 is close to type I with a very small capillary condensation step at P/P_0 = 0.4–0.6. The volume ratio of micropore to total pore detected by N_2 sorption (0.22 g cm^{-3}/0.29 g cm^{-3}, see Table 2) is ca. 76%. This implies that HCM-11 could be considered as a microporous material though it shows certain structural ordering. With an increased amount of F127, the N_2 sorption isotherms become type IV with a sharp capillary condensation step at P/P_0 = 0.6–0.7 and an H1-type hysteresis loop which is typical of cylindrical mesopores. However, sample HCM-8 with the highest concentration of F127 shows a typical IV-type isotherm with an associated H3-type hysteresis loop indicating relative wide PSDs.

The Hg intrusion data (Fig. 7d) demonstrates that HCM-8 has a high macropore volume of 3.80 cm^3 g^{-1}. Compared with previously reported results, our carbon monolith shows three times higher than that of the reported one [33]. The calculated densities of HCM-8 and HCM-2 are about 0.21 and 0.27 g cm^{-3}, respectively, which in turn verifies a high porosity of the resulting carbon monolith. By comparing the data of HCM-8 with HCM-2 (Fig. 3a), it is clear that the F127 concentration also has an effect on the total pore (or macropore) volume. The higher concentration of F127 leads to the larger total pore (or macropore) volume of the carbon product.

Furthermore, the representative SEM images of samples HCM-9 and HCM-10 (Fig. 8a and b) show that the skeletons of the carbon monoliths consist of homogeneously interconnected sphere-like units. These spherical units build up a 3-D disordered macroporous framework, with a size in the range of 8–15 μm. The SEM observations are consistent with the results of Hg porosimetry. The TEM images (Fig. 8c and d) confirm

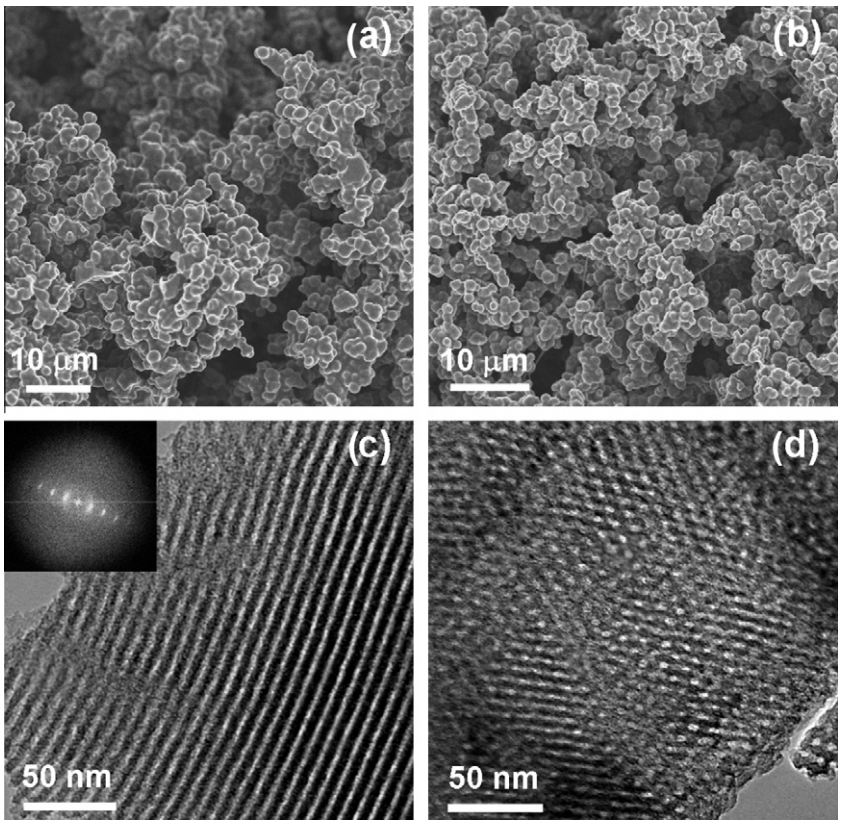

Fig. 8 – SEM images of HCM-9 (a) and HCM-10 (b), TEM image and the corresponding FFT diffractogram (inset) of HCM-9 (c), and TEM image of HCM-10 (d).

that well organized mesostructures are present in sample HCM-9 and HCM-10.

4. Conclusions

We have established a rapid and scalable synthesis of hierarchical carbon monoliths with a hexagonally array mesostructure and fully interconnected macropores. The use of base amino acid lysine as the polymerization catalyst and self-assembly promoter results in rapid gelation within 15 min at 90 °C. The polymer monoliths obtained have a robust framework, which can be dried directly in air at 50 °C without cracking. The total pore volume of the obtained carbon monoliths can be varied by changing the amount of F127 surfactant. The surface area of the carbon monolith can be increased by additional steam activation while retaining the mesostructure of the carbon. This lysine-assisted triblock-copolymer-templating method provides a direct route to fabricate the hierarchical carbon monoliths with unique features. Together with the multi-level continuous pore system and high surface area, these nitrogen-doped hierarchical carbon monoliths have potential applications in CO_2 capture, separation, capacitors and catalysis.

Acknowledgments

The project was supported by the Program for New Century Excellent Talents in University of China (NCET-08-0075), the Scientific Research Foundation for the Returned Overseas Chinese Scholars and the Ph.D. Programs Foundation (20100041110017) of Ministry of Education of China. We thank Prof. W. Zhang at Dalian Institute of Chemical Physics, Chinese Academy of Sciences, for measuring NMR.

REFERENCES

[1] Davis ME. Ordered porous materials for emerging applications. Nature 2002;417:813–21.
[2] Liang CD, Li ZJ, Dai S. Mesoporous carbon materials: synthesis and modification. Angew Chem Int Ed 2008;47:3696–717.
[3] Hu YS, Adelhelm P, Smarsly BM, Hore S, Antonietti M, Maier J. Synthesis of hierarchically porous carbon monoliths with highly ordered microstructure and their application in rechargeable lithium batteries with high-rate capability. Adv Funct Mater 2007;17:1873–8.
[4] Yuan ZY, Su BL. Insights into hierarchically meso-macroporous structured materials. J Mater Chem 2006;16:663–77.
[5] Adelhelm P, Hu YS, Chuenchom L, Antonietti M, Smarsly BM, Maier J. Generation of hierarchical meso- and macroporous carbon from mesophase pitch by spinodal decomposition using polymer templates. Adv Mater 2007;19:4012–7.
[6] Fan LZ, Hu YS, Maier J, Adelhelm P, Smarsly B, Antonietti M. High electroactivity of polyaniline in supercapacitors by using a hierarchically porous carbon monolith as a support. Adv Funct Mater 2007;17:3083–7.
[7] Lee J, Kim J, Hyeon T. Recent progress in the synthesis of porous carbon materials. Adv Mater 2006;18:2073–94.

[8] Lu AH, Schüth F. Nanocasting: a versatile strategy for creating nanostructured porous materials. Adv Mater 2006;18:1793–805.
[9] Pekala RW. Organic aerogels from the polycondensation of resorcinol with formaldehyde. J Mater Sci 1989;24:3221–7.
[10] Wan Y, Yang H, Zhao D. "Host-guest" chemistry in the synthesis of ordered nonsiliceous mesoporous materials. Acc Chem Res 2006;39:423–32.
[11] Simanjuntak FH, Jin J, Nishiyama N, Egashira Y, Ueyama K. Ordered mesoporous carbon films prepared from 1, 5-dihydroxynaphthalene/triblock copolymer composites. Carbon 2009;47:2528–55.
[12] Lin ML, Huang CC, Lo MY, Mou CY. Well-ordered mesoporous carbon thin film with perpendicular channels: application to direct methanol fuel cell. J Phys Chem C 2008;112:867–73.
[13] Rodrigue AT, Li X, Wang J, Steen WA, Fan H. Facile synthesis of nanostructured carbon through self-assembly between block copolymers and carbohydrates. Adv Funct Mater 2007;17:2710–6.
[14] Yang H, Shi Q, Liu X, Xie S, Jiang D, Zhang F, et al. Synthesis of ordered mesoporous carbon monoliths with bicontinuous cubic pore structure of Ia3d symmetry. Chem Commun 2002:2842–3.
[15] Lu AH, Smått JH, Lindén M. Combined surface and volume templating of highly porous nanocast carbon monoliths. Adv Funct Mater 2005;15:865–71.
[16] Schüth F. Endo- and exotemplating to create high-surface-area inorganic materials. Angew Chem Int Ed 2003;42:3604–22.
[17] Wang X, Bozhilov KN, Feng P. Facile preparation of hierarchically porous carbon monoliths with well-ordered mesostructures. Chem Mater 2006;18:6373–81.
[18] Wang Z, Stein A. Morphology control of carbon, silica, and carbon/silica nanocomposites: from 3D ordered macro-/mesoporous monoliths to shaped mesoporous particles. Chem Mater 2008;20:1029–40.
[19] Fang Y, Gu D, Zou Y, Wu Z, Li F, Che R, et al. A low-concentration hydrothermal synthesis of biocompatible ordered mesoporous carbon nanospheres with tunable and uniform size. Angew Chem Int Ed 2010;49:7987–91.
[20] Tanaka S, Doi A, Nakatani N, Katayamaa Y, Miyakea Y. Synthesis of ordered mesoporous carbon films, powders, and fibers by direct triblock-copolymer-templating method using an ethanol/water system. Carbon 2009;47:2688–98.
[21] Zhang F, Meng Y, Gu D, Yan Y, Yu C, Tu B, et al. A facile aqueous route to synthesize highly ordered mesoporous polymers and carbon frameworks with Ia3d bicontinuous cubic structure. J Am Chem Soc 2005;127:13508–9.
[22] Liang CD, Hong KL, Guiochon GA, Mays JW, Dai S. Synthesis of a large-scale highly ordered porous carbon film by self-assembly of block copolymers. Angew Chem Int Ed 2004;43:5785–9.
[23] Tanaka S, Nishiyama N, EgashiraY, Ueyama K. Synthesis of ordered mesoporous carbons with channel structure from an organic–organic nanocomposite. Chem Commun 2005; 2125–7.
[24] Meng Y, Gu D, Zhang F, Shi Y, Yang H, Li Z, et al. Ordered mesoporous polymers and homologous carbon frameworks: amphiphilic surfactant templating and direct transformation. Angew Chem Int Ed 2005;44:7053–9.
[25] Meng Y, Gu D, Zhang F, Shi Y, Cheng L, Feng D, et al. A family of highly ordered mesoporous polymer resin and carbon structures from organic to organic self-assembly. Chem Mater 2006;18:4447–64.
[26] Liu CY, Li LX, Song HH, Chen XH. Facile synthesis of ordered mesoporous carbons from F108/resorcinol–formaldehyde composites obtained in basic media. Chem Commun 2007:757–9.
[27] Jin J, Nishiyama N, Egashira Y, Ueyama K. Vapor phase synthesis of ultrathin carbon films with a mesoporous monolayer by a soft-templating method. Chem Commun 2009:1371–3.
[28] Tanaka S, Katayama Y, Tate MP, Hillhouse HW, Miyake Y. Fabrication of continuous mesoporous carbon films with face-centered orthorhombic symmetry through a soft templating pathway. J Mater Chem 2007;17:3639–45.
[29] Lu AH, Spliethoff B, Schüth F. Aqueous synthesis of ordered mesoporous carbon via self-assembly catalyzed by amino acid. Chem Mater 2008;20:5314–9.
[30] Liang CD, Dai S. Synthesis of mesoporous carbon materials via enhanced hydrogen–bonding interaction. J Am Chem Soc 2006;128:5316–7.
[31] Wang X, Liang CD, Dai S. Facile synthesis of ordered mesoporous carbons with high thermal stability by self-assembly of resorcinol-formaldehyde and block copolymers under highly acidic conditions. Langmuir 2008;24:7500–5.
[32] Liang C, Dai S. Dual phase separation for synthesis of bimodal meso-/macroporous carbon monoliths. Chem Mater 2009;21:2115–24.
[33] Huang Y, Cai H, Feng D, Gu D, Deng Y, Tu B, et al. One-step hydrothermal synthesis of ordered mesostructured carbonaceous monoliths with hierarchical porosities. Chem Commun 2008:2641–3.
[34] Liu F, Li C, Ren L, Meng X, Zhang H, Xiao FS. High-temperature synthesis of stable and ordered mesoporous polymer monoliths with low dielectric constants. J Mater Chem 2009;19:7921–8.
[35] Shao Y, Sui J, Yin G, Gao Y. Nitrogen-doped carbon nanostructures and their composites as catalytic materials for proton exchange membrane fuel cell. Appl Catal B Environ 2008;79:89–99.
[36] Hulicova-Jurcakova D, Seredych M, Lu GQ, Bandosz TJ. Combined effect of nitrogen- and oxygen-containing functional groups of microporous activated carbon on its electrochemical performance in supercapacitors. Adv Funct Mater 2009;19:438–47.
[37] Stein A, Wang Z, Fierke MA. Functionalization of porous carbon materials with designed pore architecture. Adv Mater 2009;21:265–93.
[38] Pevida C, Drage TC, Snape CE. Silica-templated melamine–formaldehyde resin derived adsorbents for CO_2 capture. Carbon 2008;46:1464–74.
[39] Thote JA, Iyer KS, Chatti R, Labhsetwar NK, Biniwale RB, Rayalu SS. *In situ* nitrogen enriched carbon for carbon dioxide capture. Carbon 2010;48:396–402.
[40] Hao GP, Li WC, Qian D, Lu AH. Rapid synthesis of nitrogen-doped porous carbon monolith for CO_2 capture. Adv Mater 2010;22:853–7.
[41] Metelkina O, Schubert U. Reaction of metal alkoxides with lysine: substitution of alkoxide ligands vs. lactam formation. Monatsh Chem 2003;134:1065–9.
[42] Lund-Katz S, Ibdah J, Letizia J, Thomas M, Phillips M. A ^{13}C NMR characterization of lysine residues in apolipoprotein B and their role in binding to the low density lipoprotein receptor. J Biol Chem 1988;263:13831–8.
[43] Liu YR. One-pot route to synthesize ordered mesoporous polymer/silica and carbon/silica nanocomposites. Micropor Mesopor Mater 2009;124:190–6.
[44] Mueller A, O'Brien DF. Supramolecular materials via polymerization of mesophases of hydrated amphiphiles. Chem Rev 2002;102:727–57.
[45] van Bommel KJC, Friggeri A, Shinkai S. Organic templates for the generation of inorganic materials. Angew Chem Int Ed 2003;42:980–99.